

PRELIMINARY STUDIES OF CHARGE CARRIER\*  
TRANSPORT IN MERCURIC IODIDE RADIATION DETECTORS

Jorge Llacer and Michael M. K. Watt  
 Laboratory of Nuclear Medicine and Radiation Biology  
 and Department of Electrical Sciences and Engineering  
 University of California, Los Angeles, California

and

M. Schieber, R. Carlston and W. Schnepfle  
 E.G.&G., Inc., Santa Barbara Division  
 Goleta, California

EGG-565-120

CONF-73112-23

NOTICE

This report was prepared as an account of work sponsored by the United States Government. Neither the United States nor the United States Atomic Energy Commission, nor any of their employees, nor any of their contractors, subcontractors, or their employees, makes any warranty, express or implied, or assumes any legal liability or responsibility for the accuracy, completeness or usefulness of any information, apparatus, product or process disclosed, or represents that its use would not infringe privately owned rights.

Abstract

Mercuric iodide single crystals have been grown by static and dynamic sublimation methods. Characteristics of contacts and detector capacitance have been studied by photon excitation methods. Gamma and X-ray spectrometry has been carried out with completed detectors showing resolutions comparable to the best results published to date. A measurement of hole trapping length has been made from the spectral shapes observed and has been found to be approximately 0.3 mm. Transient waveform analysis with alpha-particle excitation shows hole mobilities of approximately  $3 \text{ cm}^2/\text{V-sec}$  for a highly purified crystal and 0.05 for an expected less pure crystal. Electron mobilities of  $120 \text{ cm}^2/\text{V-sec}$  are observed. An attempt is made to explain the observed transient waveforms in terms of a single dominant trap model, with only partial success. Due to the strongly excitonic character of the material, it is proposed that the unfamiliar observations made regarding transport properties with the  $\text{HgI}_2$  detectors studied may be due to exciton dissociation under high electric fields, to long exciton lifetimes and to interactions between excitons and trapping centers in the material.

Introduction

The feasibility of using mercuric iodide as a low energy gamma and X-ray spectrometer has been unequivocally demonstrated by Malm<sup>1</sup> and by Swierkowski, Armantrout and Wichner,<sup>2</sup> following initial work by Willig and Roth.<sup>3</sup> Substantial resolution was achieved by irradiating the negative electrode of a detector so that electrons, found to be less readily trapped than holes, were responsible for most of the charge collection. Malm<sup>1</sup> has reported an electron mobility of  $70 \text{ cm}^2/\text{V-sec}$  with a limiting drift velocity of  $6.5 \times 10^5 \text{ cm/sec}$  and a hole mobility of approximately  $4 \text{ cm}^2/\text{V-sec}$ . Relevant physical constants and some trapping parameters for  $\text{HgI}_2$  are included in the first two referenced papers. In an effort to develop  $\text{HgI}_2$  to its full capabilities as a radiation detector (i.e., not limited to low energy photons), a program of purification, crystal growth and detector physics of  $\text{HgI}_2$  has been initiated. In this paper, the first results of studies on detector performance and carrier transport phenomena in crystals grown by two somewhat different processes will be reported. A discussion on crystal growth methods will also be given.

From the detector physics point of view, it is expected that this paper will raise some questions which are not readily answerable. It is strongly felt, however, that further work on the subject will lead to clear indications on how best to carry out the purification, crystal growth and detector fabrication steps for results beyond the ones that have been attained to date.

\*Work supported by the U.S. Atomic Energy Commission, Div. of Biomedical & Environmental Research, Contract AT(04-1)-GEN-12, Div. of Military Applications Contract AT(29-1)-565.

The Excitonic Nature of  $\text{HgI}_2$

Mercuric Iodide has received substantial attention in the literature of Physics on account of two of its characteristics: (1) high photoconductivity,<sup>4</sup> and (2) the strongly excitonic nature of its light absorption and emission characteristics.<sup>5-12</sup> In fact, the well-proven correlation between high photoconductivity and strong excitonic nature of materials such as  $\text{CdS}$ ,  $\text{Cu}_2\text{O}$ ,  $\text{HgI}_2$ , etc. aided the experimental establishment of the existence of the exciton.<sup>5</sup> Excellent articles on the exciton and its photoelectronic manifestations can be found in References 7 and 10. A simplified summary of the above referenced literature with regard to  $\text{HgI}_2$  can be given as follows:

1. When optical transmission measurements are made with  $\text{HgI}_2$  at low temperatures, a strong absorption peak due to exciton formation appears at photon energies somewhat less than the band gap energy. Other peaks also appear at photon energies higher than the band gap energy.
2. Measurements of photoconductivity under proper conditions show a peak of conduction when the sample is illuminated with light of the same photon energy as the one for exciton formation.
3. The bound electron-hole pair forming the exciton is not expected to dissociate thermally in substantial numbers at temperatures up to, and including, room temperature. It is more likely, however, that the exciton can dissociate by giving its energy to a trapped electron, for example, which can then become a conduction electron.
4. Electric fields in the vicinity of  $25 \text{ kV/cm}$  have been shown to force dissociation of excitons<sup>10</sup> leaving the electrons and holes free for conduction.
5. Excitons appear in three bands in  $\text{HgI}_2$ , corresponding to excitations originating in three distinct valence bands. The higher energy bands (green) have been shown to consist of excitons with lifetimes shorter than  $5 \times 10^{-10}$  seconds. The yellow and red bands have longer lifetimes (from nanoseconds to microseconds, depending on temperature).<sup>8</sup>
6. At room temperature, the excitonic peaks broaden up considerably and merge with the fundamental absorption edge, while still retaining the excitonic character.

The above facts are being emphasized strongly in this paper because it is expected that the excitonic nature of  $\text{HgI}_2$  (and a few other high-Z detector materials which could be of interest) will determine some of the basic characteristics of the material as a radiation detector. In fact, it is proposed that the final electron states occupied by the thermalized electrons

**MASTER**

## **DISCLAIMER**

**This report was prepared as an account of work sponsored by an agency of the United States Government. Neither the United States Government nor any agency Thereof, nor any of their employees, makes any warranty, express or implied, or assumes any legal liability or responsibility for the accuracy, completeness, or usefulness of any information, apparatus, product, or process disclosed, or represents that its use would not infringe privately owned rights. Reference herein to any specific commercial product, process, or service by trade name, trademark, manufacturer, or otherwise does not necessarily constitute or imply its endorsement, recommendation, or favoring by the United States Government or any agency thereof. The views and opinions of authors expressed herein do not necessarily state or reflect those of the United States Government or any agency thereof.**

## **DISCLAIMER**

**Portions of this document may be illegible in electronic image products. Images are produced from the best available original document.**

after an interaction with energetic nuclear or X-ray radiation are excitonic in great part. We shall return to this point when attempting to interpret the preamplifier output waveforms from  $\alpha$ -particle bombardment of  $\text{HgI}_2$  detectors.

### Crystal Growth

The starting material used in the present investigation has been Baker's Analyzed  $\text{HgI}_2$  (99.4% pure). The material is contaminated mainly with amorphous carbon. It is purified by either one or a combination of several steps such as molten zone refining, highly purified solvent extraction, or repeated sublimation.

A commercial Fisher Zone refiner has been used to purify lots of about 100 gr. of  $\text{HgI}_2$ , even though the high vapor pressure of 30 Torr at the melting point gives some material transport out of the zone. This transport is limited by narrowing the width of the molten zone to 1.5 mm in a 15 cm long, 1.5 cm. diameter sealed ampoule. The Pyrex or quartz tube containing the charge is evacuated to  $10^{-5}$  Torr and heated uniformly to 270°C to melt the powder. The contracted volume of the molten  $\text{HgI}_2$  is then sealed off again so as to minimize the free unoccupied volume of the ampoule. The Zone Refiner is operated vertically and contains two heating coils. About 50 passes during a period of 5 days of the two hot zones is sufficient to separate the black carbon residue which accumulates at the ends of the tube. The purified material in the center of the tube has a much lighter color.

Solvent soxhlet extraction with highly purified  $\text{CH}_3\text{OH}$  or  $\text{CH}_3\text{I}$  also separates the amorphous carbon from  $\text{HgI}_2$ . About 2.5 grams of  $\text{HgI}_2$  can be extracted by boiling about 200 ml. of solvent for 24 hours.

Repeated sublimation remains the most powerful technique to purify  $\text{HgI}_2$ . The sublimation experiments have been performed under a vacuum of  $10^{-5}$  Torr in various sized tubes from about 4 mm. to about 50 mm. internal diameter. Various temperature differentials have been used. The temperature varied from about 135 to 200°C for the hot sublimation zone and from 120 to about 30°C for the cold crystallization zone. All crystals of  $\text{HgI}_2$  which did undergo the  $\beta$ -yellow to  $\alpha$ -red phase transformation in the solid state were fragile, feather-like platelets or needles. Repeated sublimation has been performed by either using sealed long tubes in a two-zone furnace and sealing off the end part containing the residue, or by carefully removing the sublimed crystals and introducing them in a new tube. It has been found that three cycles of sublimation is the minimum number required to prepare  $\text{HgI}_2$  which does not leave any residue. The exact number of cycles depends on the amount of material per unit volume and the vacuum in the evaporation tube, i.e., the lesser the amount of material to be sublimed and the higher the vacuum, the smaller the number of cycles in repeated sublimation needed for not leaving any black residue. The sublimation purified material has a much lighter red color than that of material purified by other methods, even in the polycrystalline stage.

Crystal growth has been performed by a static sublimation method similar to that described for purification by sublimation. The size of the largest grown crystals is 3 x 3 x 4 mm. Larger ingots of  $\text{HgI}_2$ , as shown in Figure 1, have been grown using a "pulling from the vapor" method. The purified material is enclosed in a tube, which is then evacuated and sealed. The tube is introduced in a furnace with a temperature gradient and the growing crystal is withdrawn at rates between 0.5 and 1.0 mm/hour. A typical size for an ingot is 6 to 7 mm. diameter and 25 to 35 mm. long. At this writing, most of the ingots grown have substantial

single crystal sections. The one shown in Figure 1, for example, is a single crystal for almost 1 cm. of length from left hand tip. Work is in progress to improve this growth method. A more detailed description of crystal growth methods will be published elsewhere.<sup>13</sup>

### Detector Fabrication

#### a. Crystal Handling

Initial work on some of the electrical and optical characteristics of  $\text{HgI}_2$  was carried out with crystals provided by R. Willig, of the Siemens Research Laboratory. In particular, two crystals apparently grown from solution, but which contained no visible inclusions or occlusions, were studied in some detail. They were labelled S-1 and S-2. It soon became apparent that  $\text{HgI}_2$  crystals are quite fragile and that handling had to be done with plastic-ball tipped tweezers. The weakly bound layers perpendicular to the c-axis of the crystal can be cleaved neatly. A properly grown cleaved crystal will be completely transparent (not just translucent) when looking through the cleaved surfaces.

Crystals grown by E.G. & G., Santa Barbara Division, are designated EGG with a suffix to internally identify the growth parameters. Detectors EGG-2-1 (a) and (b), about which we report here, were obtained by cleaving from a larger piece of material grown by the simple static sublimation method indicated above. Detector EGG-HD-1-3, also to be discussed below, was cleaved from a single crystal portion of an ingot "pulled from the vapor". In all cases, removal of external damage has been effected by etching or dissolving in Methanol, Electronic Grade, and drying in filtered dry  $\text{N}_2$ . Progress is being made on cutting and lapping slices obtained from ingots, with a view to an ultimately more practical fabrication method.

#### b. Contacts

Like practically every worker in the field, we have used Aquadag contacts painted on the surfaces chosen for the electrodes. A brief study of the properties of this contact has been made in order to ascertain some of its properties. Dark currents of the order of picoamps with voltages of up to several hundred volts have usually been encountered with good crystals of mm. dimensions. Erratic fluctuations with S-1 and S-2 crystals, not allowing any systematic measurements of dark current and contact characteristics, indicated the convenience of carrying out photoconductance measurements. Photons with a wavelength of 5900 Å corresponding to the peak of photoconduction were used to illuminate uniformly the exposed edge of crystal S-2. Light intensity was adjusted to produce currents in the nanoampere region, with potentials up to 500 volts. I-V characteristics were moderately linear from 10 to 500 volts, but with differing slopes by a factor of nearly two upon polarity reversal. Another useful item of information which was extracted from the measurement was the failure of the I-V lines to aim towards the origin of coordinates. This prompted us to make a careful measurement of I-V characteristics at low voltage levels. Light of a longer wavelength (6750 Å), corresponding to the beginning of the absorption edge, was chosen in order to generate carriers more uniformly over the whole crystal volume. The I-V results are shown in Figure 2. The characteristic resembles very much what one would obtain for two diodes back to back. A simplified schematic of a low bias situation is also depicted in Figure 2. Electron-hole pairs generated by light find no difficulty in "falling into" their attracting carbon contacts, but there is a barrier at the opposite sides for replenishing of charge carriers.

A quasi-linear increase of current with potential at higher bias would indicate, then, that the barrier breaks down or effectively decreases in height under such conditions, i.e., the contacts become practically ohmic. Low level current is then limited by carrier generation and applied field.

The question of whether the carbon contacts can take up most of the applied voltage, leaving large regions of the crystal without field can be answered negatively: in the absence of large number of traps in the band gap, there are not enough bound charges in the HgI<sub>2</sub> material to terminate fields (high resistivity material). The field is also found to reach the opposite contact in order to create barrier breakdown. The existence of the "S" like curve in the low voltage I-V characteristic does indicate, however, the existence of some fields in the device at equilibrium. In fact, shining light on the edge of an unbiased crystal near one of the contacts causes positive current out of that contact, confirming the existence of a barrier that can support a potential. The presence of large numbers of traps could modify the picture considerably, but the transient waveform analysis discussed below appears to rule out gross non-uniformities in the field distribution.

### c. Mounting

EGG crystals have been mounted on a round glass substrate and held in place by a drop of Aquadag on a metallic evaporated strip. The second contact was a thin wire again held in place with Aquadag, terminating on a drop of silver epoxy on the substrate (See Figure 3). All three EGG crystals whose characteristics will be reported here have been mounted several times, with intervening etching to improve leakage current characteristics, when necessary, or for thinning down. Contrary to the practice of the Livermore group,<sup>2</sup> the Aquadag contacts have been made to cover the entire surface of the crystal planes (perpendicular to c-axis) for the purpose of obtaining more uniform fields for charge collection studies. It must be indicated, though, that repeated handling in some cases resulted in irreversible damage to the crystals.

## Device Characteristics and Performance

### a. Leakage Current

Finished devices which have been successful radiation detectors exhibit leakage currents which decrease with time after initial application or increases of bias. Crystals EGG-2-1 have required slow increments of 50 to 100 volts over periods of as much as 24 hours in order to obtain currents of a few picoamps at 1000 or more volts. Once the proper "condition" has been established, bias can be removed, the crystal exposed to light, and even after periods of as much as perhaps 30 minutes one can reapply high bias without much delay in obtaining low currents. Crystal EGG-HD-1-3 has not required such long delays, and it has been usually ready to operate almost immediately after application of bias. Concurrently with the time-current effects, the ability of crystals to show good charge collection characteristics is also time dependent. The EGG-2-1 series crystals do not reach a final stable pulse height for a monochromatic source under fixed bias until 24 to 48 hours after the first application of bias. Crystal EGG-HD-1-3 works well immediately. These differences could be due to an expected much higher level of purity of the HD crystal in comparison with the 2-1 series due to cleaner growth methods. Crystals which fail to allow the application of high enough fields for good charge collection usually exhibit currents which are stable

above 10 or 20 picoamps at low voltages, and which tend to increase with time at higher bias. It is suspected that structural damage due to excessive handling or violent cleaving or cutting is the cause of these effects. Annealing experiments have not yet been carried out on these samples.

### b. Capacitance

Dark capacitance versus frequency measurements have been carried out only on the two Siemens crystals. S-1, which exhibited internal structural damage when seen in a microscope with transmitted light, showed a substantial dark capacitance increase by lowering the measurement frequency from 100 kHz to 10 Hz. Crystal S-2, which was handled with much more care, showed a completely flat dark capacitance versus frequency characteristic within the accuracy of the measurement (a few per cent). With a correction for stray capacitance, the relative dielectric constant for fields perpendicular to the c-axis is found to be approximately 8. Swierkowski, et. al.<sup>2</sup> have found a value of 8.8 to 9.8 for fields parallel to the c-axis. The difference between the two Siemens crystals is attributable to polarization at trap sites due to physical damage of the crystal, requiring trapping and detrapping of carriers which can only follow low frequencies.

Another interesting measurement which may lead to future sensitive measurements of trapping properties in HgI<sub>2</sub> is that of photoconductance and photocapacitance as a function of the frequency of the alternating voltage applied to the terminals. Crystal S-2 was used for these measurements. Monochromatic light with a wavelength of 7500 Å (deeply penetrating) was allowed to excite the crystal from the edge. A Princeton Applied Research phase locked detector was used to measure conductance and capacitance as a function of frequency. Accurate calibration of phase was carried out at each point with a ceramic 1 pfd. capacitor. Figure 4 shows the results obtained. The frequency of the voltage signal is designated  $f_r$ . The magnitude was 1 volt RMS. A simple minded interpretation of the results can be given as follows: Carrier pairs are being generated more or less uniformly throughout the crystal volume. In the absence of trapping, the carriers would follow the applied voltage in exact phase (considering the low frequencies of the measurement). The only 90° phase current would then be the displacement current, giving a capacitance equal to the dark capacitance. In the presence of trapping, however, a lag in the current due to slow detrapping of charge carriers can be expected and, as the frequency of the applied voltage is decreased, the larger the net polarization of the material becomes. Qualitatively, one can also expect that the photoconductance will be lower at low frequency due to a decreased availability of untrapped carriers. These are only tentative explanations. A whole body of literature exists on photocapacitance, but the technique is only indicated here as a possible means to study trapping in HgI<sub>2</sub>.

### c. Gamma and X-ray Spectrometry

Spectra from some standard sources have been obtained with crystals EGG-2-1a) and EGG-HD-1-3. Both of them have active areas of the order of 5 mm<sup>2</sup>. The 2-1 crystal is 0.75 mm in thickness, while the HD crystal is 0.1 mm thick. Maximum applicable bias has been 2000 and 450 volts respectively. The detector entrance surface has always been biased negatively. Figures 5 and 6 show the results obtained for a <sup>241</sup>Am source, collimated to a beam of approximately 1.0 mm diameter at the detector surface, obtained from the thick and the thin detectors respectively. The substantial difference in appearance of the spectra is mainly due to

the different relative efficiency for photoelectric interactions of the 59.5 keV gamma rays. Thus, in Figure 5, the Np X-rays of the source are barely discernible in the long tail caused by hole trapping. It must also be pointed out that the source encapsulation resulted in a reduction in the number of Np X-rays emitted by a factor of 6 with respect to standard sources, as remarked by Swierkowski.<sup>14</sup> In Figure 6, the Np X-rays are the most prominent feature of the spectrum. It is believed that the "background" counts under the X-ray lines are not so much due to hole trapping but to scattered radiation in the test chamber, as most of the 59.5 gamma rays are transmitted by the HgI<sub>2</sub> crystal. An interesting feature of both spectra is the 31 keV K<sub>α</sub> escape peak from Iodine, corresponding to photoelectric interactions of the 59.5 keV line creating an X-ray fluorescence photon at an Iodine atom which manages to leave the crystal without interacting in it. The energy of this escape peak is, therefore, 59.5 - K<sub>α</sub> energy for Iodine. The relative intensity of this line with respect to the main 59.5 keV line is expected to increase as the detector is made thinner because of a higher probability of escape of the K<sub>α</sub> X-ray of Iodine. This is confirmed by comparison of the two spectra. Another peak at 28.5 keV appears also in Figure 5, at precisely the K<sub>α</sub> energy of Iodine. We believe that this peak corresponds to X-ray fluorescence of the Iodine in the detector with the escape of the 31 keV hot electron. This requires that such interactions be exclusively limited to essentially surface events. Such a peak is not clearly observable in Figure 6, and the reason for this is not very clear at this time. It has been ascertained without doubt that the peak in question is not the K<sub>β</sub> escape peak of Iodine, which would appear about 2 keV below the observed one and would also be expected to be much smaller than the K<sub>α</sub> escape peak.

Figure 7 shows a spectrum obtained from a <sup>57</sup>Co source in a Pb holder with detector EGG-2-1a). The fluoresced Pb X-rays are very prominent, as the crystal is substantially more efficient at 74 keV than at 122 keV. Strong hole trapping effects at the high energies and, it is believed, a great deal of radiation scattered in the chamber are observable. Hg and I escape peaks are to be found, and there are a few unexplained ones. Because of a substantial pulse height defect at the higher energies (hole trapping), a very precise energy calibration has not been carried out, and some of the identifications in the figure are tentative.

Upon observing Figure 7, the reader might well ask about the possible usefulness of a HgI<sub>2</sub> detector in doing spectrometry of an unknown source. It is felt by the authors that a perfected and well understood HgI<sub>2</sub> detector, giving sharp peaks (not like the present ones), can be almost as useful in such a situation as a Germanium detector. The extra pain necessary to unravel the results may be the payment exacted for having a high resolution and high efficiency detector operable in air at room temperature. Obviously, in other situations where the source is known, no real problem is presented.

In order to complete the record, a <sup>55</sup>Fe spectrum has also been obtained with crystal HD and is shown in Figure 8. Scattering through the source Mylar covering and the graphite contact of the detector may give rise to the shoulder behind the peak. The effects of the time constant  $\tau$  of the pseudo-Gaussian filter used in the main amplifier have been investigated with crystal 2-1 operated at 2000 volts. A commercial amplifier has been modified to provide values of  $\tau$  of up to 96  $\mu$  sec., and an appropriate sampling circuit with a linear gate has been set up in order to generate

signals acceptable to a pulse height analyzer.<sup>15</sup> A flat topped pulser with a duration of over 1 msec. was used to provide gain calibration when changing the time constant. The results obtained are shown in Figure 9. An increase in pulse height is quite evident with longer values of  $\tau$ , even at the high values used. Slow hold detrapping can be blamed for this performance. Although it is not clear from the reproduced spectra, the K<sub>α</sub> Iodine escape peak ceased to shift to higher channel number at values of  $\tau$  equal to 64  $\mu$ sec. or larger. Since these interactions are quite superficial and considerably more numerous near the entrance surface of the detector, they correspond to almost purely electron traversal events. Therefore, the position of the 31 keV peak at 96  $\mu$ sec. has been chosen as the full collection calibration point for determining the mean energy for formation of an electron-hole pair in HgI<sub>2</sub>, at least at fields of 26.6 kV/cm. The importance of this remark will become clear below.

By measuring the calibration capacitance of the preamplifier as carefully as possible "in situ" and using standard techniques, it has been found that the mean energy for electron-hole pair formation is 4.9 eV with a few per cent error expected. Reference 2 gives a value of 4.33, in moderate agreement.

#### d. Hole Trapping Length

The above interpretation of the lack of shifting of the 31 keV peak at 64 and 96  $\mu$ sec. time constants leads to the conclusion that the spectrum of Figure 9 for  $\tau = 96$  sec. corresponds to full collection of electrons for all gamma ray interactions. Peak shape and location is then due to limited collection due to hole trapping and to a long detrapping time. For a crystal of thickness  $d$  with full electron collection and hole collection limited by a trapping length  $L_t$ , a localized gamma ray interaction occurring at a depth  $x$  from the entrance surface will result in a total collected charge

$$Q(x) = \frac{Q_0}{d} \left\{ (d-x) - L_t [1 - \exp(-x/L_t)] \right\} \quad (1)$$

where  $Q_0$  is the total charge liberated at  $x$ . The first term in the brackets corresponds to the fraction of induced charge due to electron motion and the second to hole motion. This relation can be derived easily from the basic considerations of Day, Dearnaley and Palms.<sup>15</sup> For low energy gamma rays entering the crystal at  $x = 0$ , the probability that a photoelectric interaction occurs at a distance  $x$  in an interval  $dx$  is

$$P(x) dx = \mu_{ph} \exp(-\mu_{ph} x) dx$$

where  $\mu_{ph}$  is the photoelectric absorption coefficient. A plot of  $P(x)$  versus  $Q(x)$ , interpreted as number of counts versus energy in a standard spectrum, has been made for several values of  $L_t$  and it is shown in Figure 10.  $Q_0$  has been set at the expected position for the 59.5 keV peak. The real crystal thickness  $d$  and the absorption coefficient for 59.5 keV gamma rays have been used as parameters for the calculation. The only adjustment has been the normalization of the spectrum height to the experimental curve for  $\tau = 96$   $\mu$ sec of Figure 9, also shown, at a point corresponding to approximately 50 keV. Considering the effect of convolution with a Gaussian due to electronic noise, comparison of the experimental and calculated spectrum shapes indicates a trapping length of approximately 0.3 mm. for crystal EGG-2-1a) at a field of  $2.66 \times 10^4$  V/cm. This gives a mobility-lifetime product of  $1.1 \times 10^{-6}$  cm<sup>2</sup>/V for holes, in agreement with Malm.<sup>1</sup>

e. Effect of Hole Trapping Length

It is a simple but nonetheless useful result to compute the spectral shapes that can be expected from a detector with characteristics similar to those of the 2-1 material; i.e., practically full electron collection (at high enough bias and/or long enough time constants) and hole collection limited by long term trapping with a length  $L_t = 0.3$  mm. Spectral shapes are shown in Figure 11 a) and b) for photon energies up to 100 keV and thicknesses which would be considered useful for detection of the given radiation energy. The calculated shapes appear to be very much in agreement with the results published in Reference 2 and in the present paper. It must be noted that up to photon energies of 20 keV, crystal thicknesses of a few tenths of a mm. can yield quite good results, while at the higher energies, thin crystals with  $L_t$  of the order of 0.3 mm. are quite useless as spectrometers of unknown sources. In all cases, however, it is better to use a thicker crystal rather than a thinner one, so as to minimize the fraction of induced charge which has to be handled by holes (this provided that electron trapping does not become a substantial problem with thicker crystals).

f. Alpha-Particle Excitation

For the purpose of obtaining a more direct measurement of transport parameters in the HgI<sub>2</sub> crystals under study, the output waveforms of charge sensitive preamplifiers have been recorded under alpha particle excitation of the detector. A collimator of 1 mm. diameter, 3 mm. depth was used with the source in air. A total  $\alpha$ -particle path of near 0.8 cm. to the detector, plus a layer of Aquadag of unspecified thickness caused energy straggling of the particles, but well recognizable peaks still appeared in the spectrum. Although the output waveforms of the preamplifier could be analyzed fairly well with 60 keV gamma rays, it was found impossible to scan detectors along their edges and be completely sure that only electrons or holes were giving rise to signals. Scattering of gamma rays from an intense, finely collimated, <sup>241</sup>Am source in a relatively small detector chamber proved to be excessive for unambiguous results.

Two different preamplifiers were used for the measurements. One of them, described as fast, has a risetime of 15 nsec. or less, but it is moderately noisy. A second one, with 50 nsec. risetime, described as slow, was much quieter. The voltage gain of the two units is also different. Measurements with EGG-HD-1-3 (0.1 mm. thickness) biased for electron traversal are shown in Figure 12. The risetime of the signals at both 150 and 450 volts bias is limited by the risetime of the fast preamplifier. Considering that a detector risetime  $\tau_r$  of about 1/2 the amplifier risetime should begin to be observable, one can estimate  $\tau_r$  to be equal or less than  $8 \times 10^{-9}$  sec., giving an electron mobility  $\mu_e > 83$  cm<sup>2</sup>/V-sec. When the preamplifier output is observed in a longer time scale, no substantial indication of any other maxima in the waveform is observed. One can conclude, from the normal experience of Si and Ge workers, that full electron collection is occurring at 150 volts bias. However, the pulse height at 450 volts bias, also apparently fully collected, is markedly larger than at 150 volts, and the corresponding spectrum was also displaced towards higher energies. This effect is observed in all the experiments to be reported below with electrons or holes and will be discussed further at the end of the paper. In Figure 12 there is a fraction of events which appear with very low risetimes. These are due to  $\alpha$ -particles impinging on a section of the crystal which was not covered by Aquadag, and they are inconsequential.

Figure 13 shows the corresponding results for hole traversal, obtained by simply reversing the polarity of the bias and waiting a few minutes. A fast part, which is due to a substantial penetration of  $\alpha$ -particles into the detector, and is therefore electron contribution, is quite observable (the detector is only 100 microns thick). The hole contribution has a much smaller slope and the end of the transit time is quite clearly defined. From transit times measured at 150, 250, 350, and 450 volts bias, a hole mobility  $\mu_h$  of  $2.95 \pm 0.12$  cm<sup>2</sup>/V-sec is obtained. Spectral shapes for hole traversal did form a peak, but not as distinct as with electron traversal. No other maxima of the waveforms occurred at long observation times, and the dependence of maximum pulse height on applied field is also evident. Furthermore, the absolute magnitudes of the signals for electrons are substantially larger than those for holes.

Measurements were next carried out with a thicker crystal EGG-2-1b), with a thickness of 0.54 mm. Figure 14 shows the results for electron traversal at two different time scales. Fields applied were substantially lower than those used with the previous crystal. Fast and slow portions of the transient response are clearly observable. For the analysis of these results in terms of a single dominant trap characterized by a trapping time  $\tau^+$  and a detrapping time  $\tau_D$ , the treatments by J. W. Mayer<sup>17</sup> and by Zanio, Akutagawa and Kikuchi<sup>18</sup> are very useful. From the slope at the beginning of the transient one can determine the mobility. Since the fast part is practically straight, a transit time not particularly hindered by trapping can be defined. From five measurements with bias voltages between 250 and 1050 volts, an electron mobility  $\mu_e = 120 \pm 8.5$  cm<sup>2</sup>/V-sec is obtained. From the observation that half the pulse height is fast and half slow (very closely so at all voltages tested) one could make the observation that during  $\tau_r$  about half the charge generated has been trapped and it will detrapp slowly at  $t > \tau_r$ . With this assumption, a detrapping time  $\tau_D = 20$   $\mu$ secs is obtained from Figures 14 c) and d). In order to determine what value  $\tau^+$  should have in order to trap one half of the total charge in time  $\tau_r$ , Equation (5.7.10) of Reference 17 (equivalent to Equation (23) of Reference 18) can be used by requiring that at time  $\tau_r$

$$\frac{Q(\tau_r)}{q N_0} = \frac{1}{2} = \frac{\tau_e}{\tau_r} \left\{ (\tau_r/\tau_D) + (\tau_e/\tau^+) [1 - \exp(-\tau_r/\tau_e)] \right\} \quad (2)$$

with  $1/\tau_e = (1/\tau^+) + (1/\tau_D)$ . For the present case,  $\tau_D \gg \tau_r$ , while one expects  $\tau^+$  to be of the same order as  $\tau_r$ , because of substantial trapping during the transit time. It follows that  $\tau_D \gg \tau^+$  and, therefore,  $1/\tau_e = 1/\tau^+$ . With these approximations, Equation (2) is reduced to

$$\frac{Q(\tau_r)}{q N_0} = \frac{\tau^+}{\tau_r} [1 - \exp(-\tau_r/\tau^+)] \quad (3)$$

to be solved for  $\tau^+$ . It is found that no single value of  $\tau^+$  will satisfy Equation (3) for the five measurements at different voltages. A value of  $\tau^+ = 40$  nsec. is within range, but implies a change in the value of  $Q(\tau_r)/qN_0$  (the fraction collected at the end of transit time  $\tau_r$ ) from 0.19 to 0.78 for the observed range of transit time. This does not correspond to the experimental results. Furthermore, with  $\tau^+ = 40$  nsec., the fast part of the rising waveform would have a much more markedly exponential shape. Qualitatively, the point of discord is the assumption that the fast part of the waveform can be practically straight and at the same time about half of the carriers are being trapped. The main result from this discussion is that the single

trap model does not seem to apply well in this particular sample of HgI<sub>2</sub>. Once more, maximum pulse height is dependent on field (both the fast and slow parts).

Figure 15 shows results for holes in the thick crystal. Photographs a) and b) show clearly a fast part, again expected to be due to electron contribution from some deeply penetrating  $\alpha$ -particles, and the beginning of the slow transient due to holes. Photographs c) and d), in a long time scale, show hole transients with initial slopes changing very closely by a factor of two, corresponding to doubling of the field. The mobilities calculated for this crystal from those slopes are quite small,  $\mu_h = 0.05 \text{ cm}^2/\text{V-sec}$ . The low value can be due to the expected lower purity of the 2-1 crystal with respect to the HD crystal, but one must consider the possibility of structural damage creating shallow traps which limit the mobility.

The behavior of holes lends itself more easily to the single trap model characterization with  $\tau_D \gg \tau_r$  and  $\tau^+$  of the order to  $\tau_r$ . Under such conditions

$$\frac{Q(t)}{q N_0} = \frac{\tau^+ \mu E}{d} [1 - \exp(-t/\tau^+)], \quad t < \tau_r \quad (4)$$

(Equation 5.7.5, Reference 17). A simple fitting indicates a trapping time  $\tau_h^+ = 45 \mu\text{secs}$ , leading to a  $\mu_h \tau_h^+$  product of  $2.25 \times 10^{-6} \text{ cm}^2/\text{V}$  and a trapping length of 0.6 mm. for a field of  $2.6 \times 10^4 \text{ V/cm}$ . This was the field applied to crystal EGG-2-1a) for obtaining the spectrum shown in Figure 8. The trapping length obtained from that spectrum shape was 0.3 mm. Both a) and b) crystals come from the same ingot and a similarity of characteristics is expected. Some measure of consistence is, in fact, found in the obtained trapping length between the two crystals, by different methods.

### Conclusions

All the measurements described above have been carried out in the spirit of an initial investigation, so as to get acquainted with the peculiarities of HgI<sub>2</sub>. Since the material does not appear to have any inherent problems with leakage current, contacts, or anomalous dark capacitance which could affect detector performance, the transport characteristics for charge carriers, including trapping effects, remain the most important area to work on, from the detector physics point of view. As for crystal growth, a great deal remains to be done, both in purification and in single crystal technology, but much of the direction for these areas will have to come from an understanding of the relevant carrier transport phenomena.

The majority of transport parameters measured are in substantial agreement with the results of Malm,<sup>1</sup> but there is one dominant question that keeps recurring: Why do fully and/or partially collected signals, both from holes and electrons, have an amplitude which depends on field strength? If one assumes that even the better hole and electron mobilities measured are still trap limited, i.e., carriers move by constantly trapping and detrapping from shallow traps, the question is not satisfactorily answered. This would correspond to case c) in J. W. Mayer's treatment of the single level trap (p. 480, Reference 16) in which case an effective mobility  $\mu\tau^+ / (\tau_D + \tau^+)$  is found to control carrier transport. This model, which would give the straight rising wave forms found experimentally for electrons (and holes under proper conditions), still does not account for an increase in the maximum amplitudes with increasing field.

Perhaps an elaborate multiple level trap model could be devised to explain the observed result, but it

appears more reasonable to invoke the proven existence of excitons in HgI<sub>2</sub>. If a large number of the generated carriers thermalize in the form of bound electron hole pairs which can dissociate by the action of high electric fields, we may have an explanation for the field dependence of signal magnitude. Also, the observed long lifetimes for the longer wavelength excitons, as described above, could contribute to the apparent long detrapping times observed for holes and for the slow portions of electron waveforms. The observation that electron signals are usually larger than hole signals, under equal bias conditions, can also be explained in terms of exciton dissociation at an electron trap, resulting in more electrons than holes being normally available for conduction. What is being proposed is that improvement of transport in HgI<sub>2</sub> may not only be a question of searching for traps and learning how to reduce their number, but we may have to contend with the complicating factor of exciton-trap interactions. If it is proven that excitons have an important role in carrier transport, the mean energy for formation of an electron-hole pair would be voltage dependent. Studies of HgI<sub>2</sub> by transient photoinjection techniques as a function of temperature are now in preparation at our laboratory and it is expected that more concrete information will be obtained on these matters.

Whether the excitonic character of the material proves important or not, it is evident from the results reported that HgI<sub>2</sub> can become an important material for radiation detection at room temperature. Even if hole mobility remains in the vicinity of 3 or 4 cm<sup>2</sup>/Volt-sec, detection of deeply penetrating radiation with a detector of 5 mm. thickness, with 5000 volts applied, could be carried out with flat-topped filtering with durations in the order of 15 to 20 secs., as developed by Radeka.<sup>19</sup> Good resolution and reasonable count rates could be obtained provided that the apparent trapping can be reduced in the future. Uses at lower energies in nuclear medicine and radiology are contemplated as soon as larger area crystals can become routinely available.

### Acknowledgments

The authors would like to acknowledge the interest, support and advice of Mr. Gerald C. Huth, UCLA, and Dr. H. A. Lamonds, E.G.& G., the frequent technological assistance of John Ewins, UCLA, and productive discussions with S. Swierkowski of the Lawrence Livermore Laboratory.

### References

1. H.L. Malm, IEEE Trans. Nucl. Science, NS-19, No. 3, 1972, p. 263.
2. S.P. Swierkowski, G.A. Armantrout, R. Wichner, App. Phys. Lett., 23, No. 5, 1973, p. 281.
3. W.R. Willig, S. Roth, Proc. Internat. Symposium on CdTe, Siffert & Coche, Eds., Strasbourg (France), June 1971.
4. R.H. Bube, Phys. Review, 106, No. 4, May 1957, p. 703.
5. E.F. Gross and B.V. Novikov, J. Phys. Chem. Solids, 22, 1961, p. 87.
6. E.G. Gross and R.K. Shekhamet'ev, Soviet Physics, Solid State, 3, No. 10, 1962, p. 2297.
7. E.F. Gross, Soviet Physics, Uspekhi, 5, No. 2, Sept-Oct 1972, p. 195.
8. R. Klein, F. Raga and S. Nikitine, Proc. of the International Conference on Luminescence, Budapest, 1966, p. 1496.
9. S. Nikitine and R. Klein, Phys. Rev. Letters, 20, No. 4, 1966, p. 341.
10. A. Coret, Ann. Phys., t.1, 1966, p. 673.
11. A. Daunois, J.L. Deiss and S. Nikitine, Phys. Letters, 28A, No. 4, 1968, p. 274.



12. C.C. Coleman and M. Chester, *Phys. Letters*, 29A, No. 3, p. 145.
13. M. Schieber, R. Carlston, H. Lamonds, J. Llacer, P. Randke and W. Schnepfle, International Conference on Crystal Growth, Tokyo, 1973, To be published in *J. Crystal Growth*, 1974.
14. S.P. Swierkowski, private communication.
15. Method suggested by Z.H. Cho, UCLA.
16. R.B. Day, G. Dearnaley and J.M. Palms, *IEEE Trans. Nucl. Science*, NS-14, 1967, p. 487.
17. J.W. Mayer, in "Semiconductor Detectors", G. Bertolini and A. Coche, Eds., Wiley, 1968.
18. K.R. Zanio, W.M. Akutagawa and R. Kikuchi, *JAP*, 39, No. 6, 1968, p. 2818.
19. V. Radeka, *IEEE Trans. Nucl. Science*, NS-19, No. 1, 1972, p. 412.

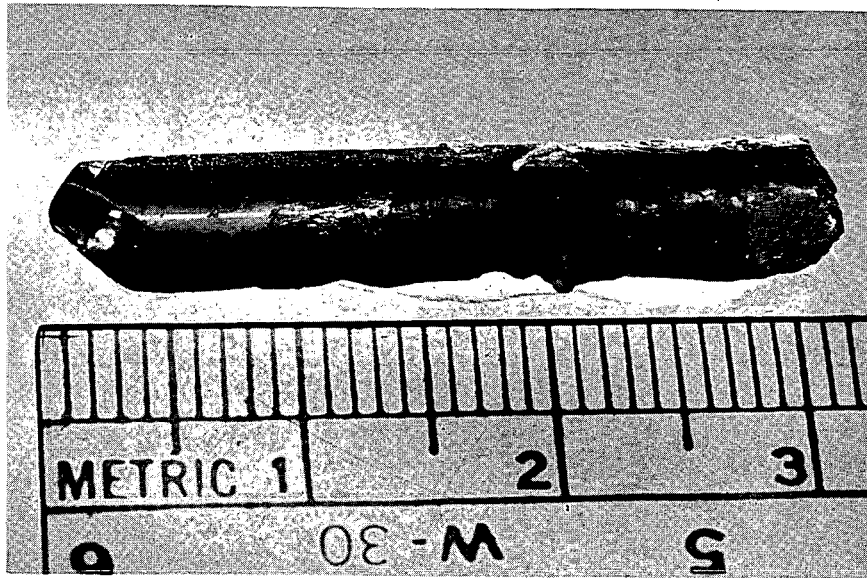


Figure 1. Ingot of  $\text{HgI}_2$  Grown by "Pulling from the Vapor" Technique. First cm. on Left Side is Practically all a Single Crystal.

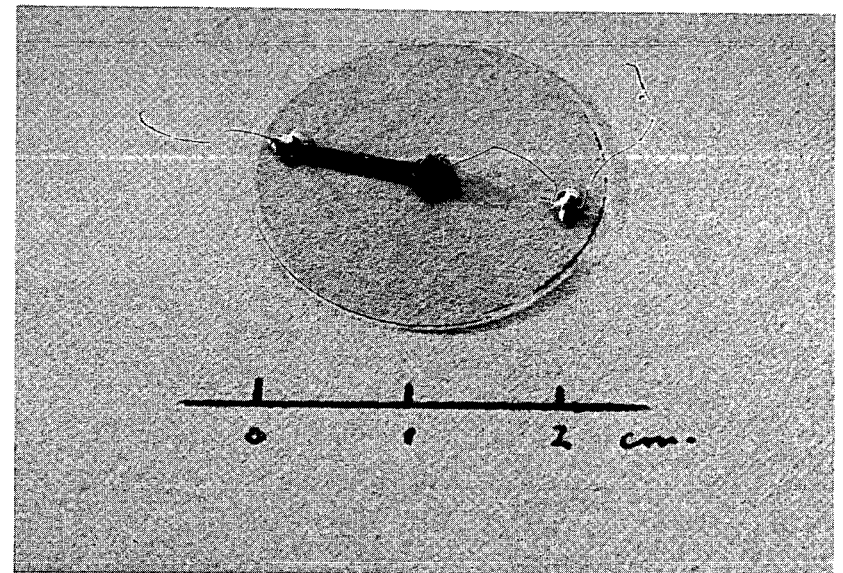


Figure 3. Crystal EGG-2-1a) Mounted on Glass Disk.

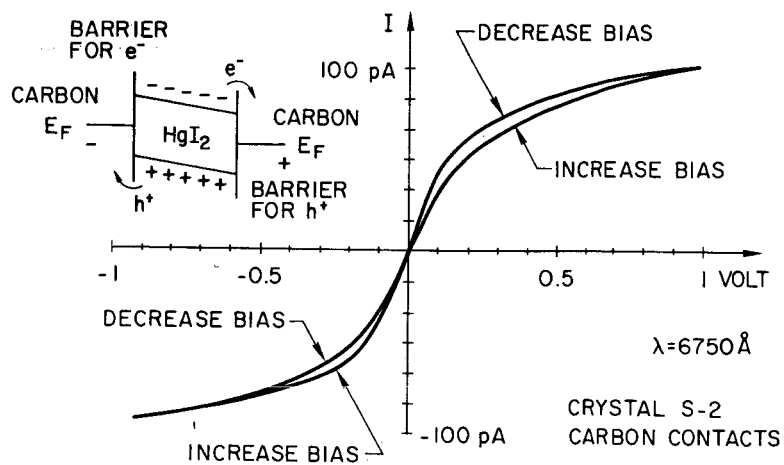


Figure 2. Low Level I-V Characteristics of a Photo-Excited Graphite- $\text{HgI}_2$ -Graphite Device.

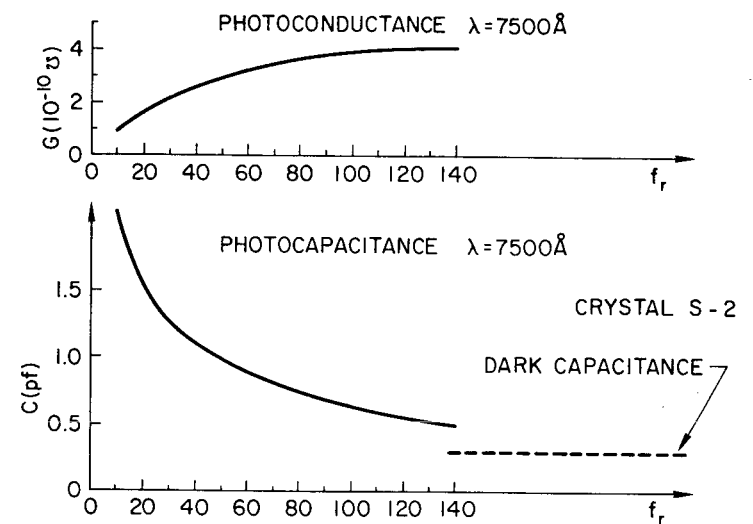


Figure 4. Photoconductance and Photocapacitance of Crystal S-2 at Low Frequencies of Applied Alternating Voltage.

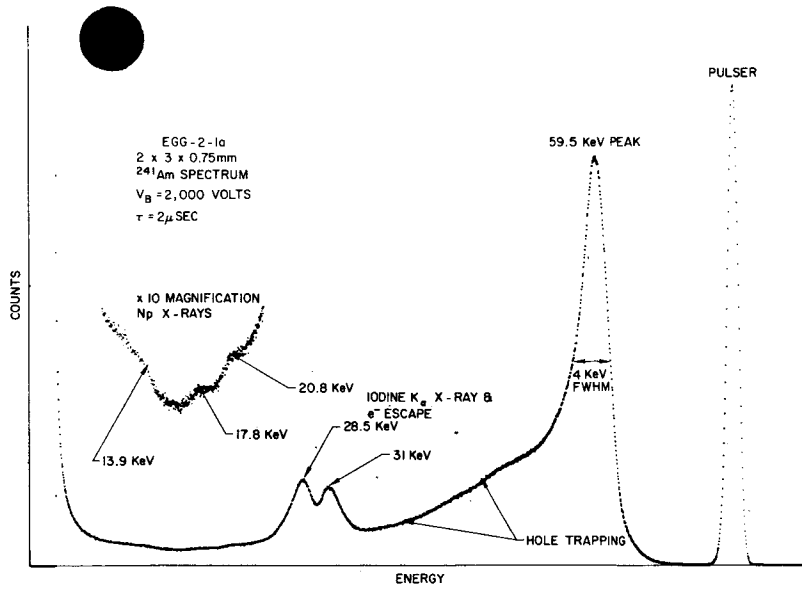


Figure 5. Spectrum of <sup>241</sup>Am Source Obtained with Crystal EGG-2-1a) (Thickness 0.75 mm.).

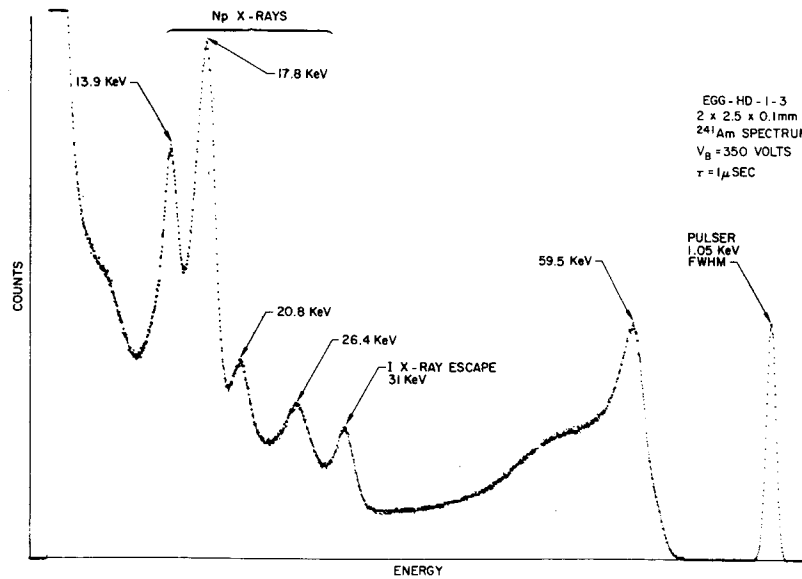


Figure 6. Spectrum of <sup>241</sup>Am Source Obtained with Crystal EGG-HD-1-3 (Thickness 0.1 mm.).

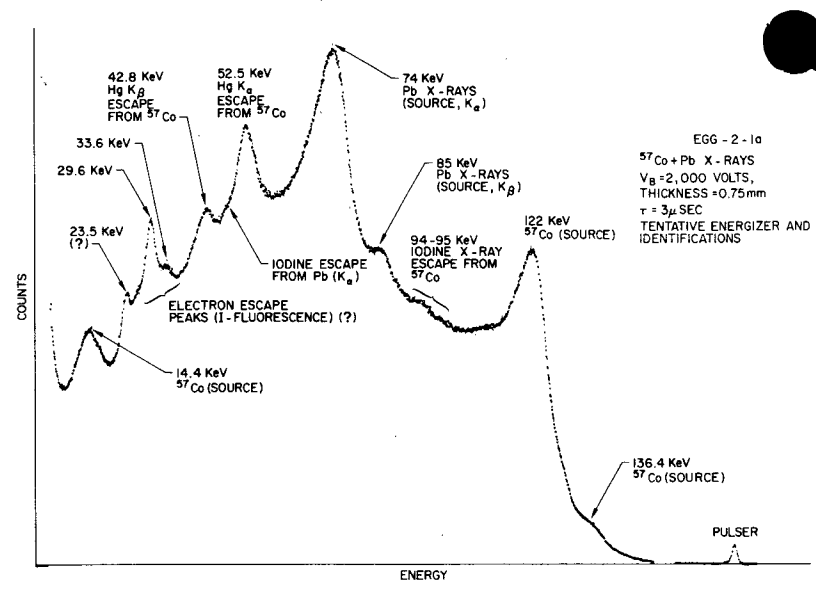


Figure 7. Compound Spectrum of <sup>57</sup>Co and X-ray Fluorescence of Pb Obtained with EGG-2-1a) Crystal.

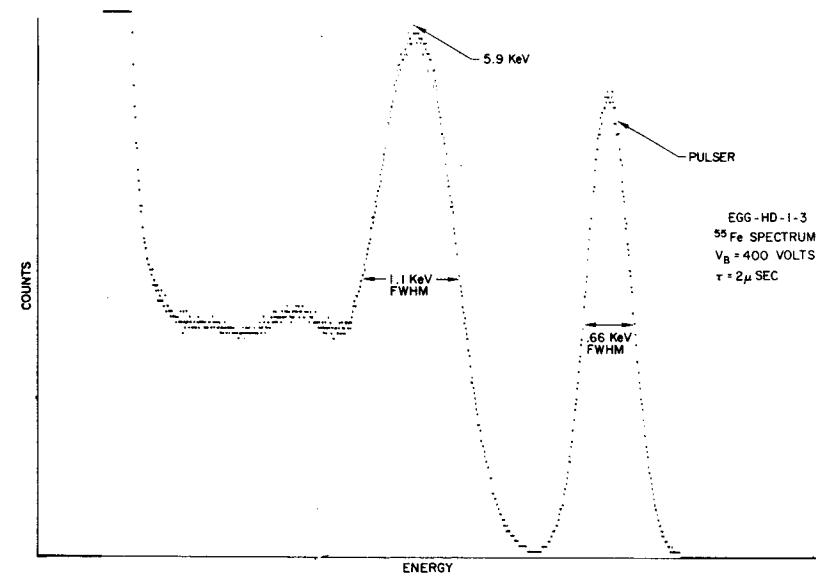


Figure 8. Spectrum of <sup>55</sup>Fe Source Obtained with Crystal EGG-HD-1-3.

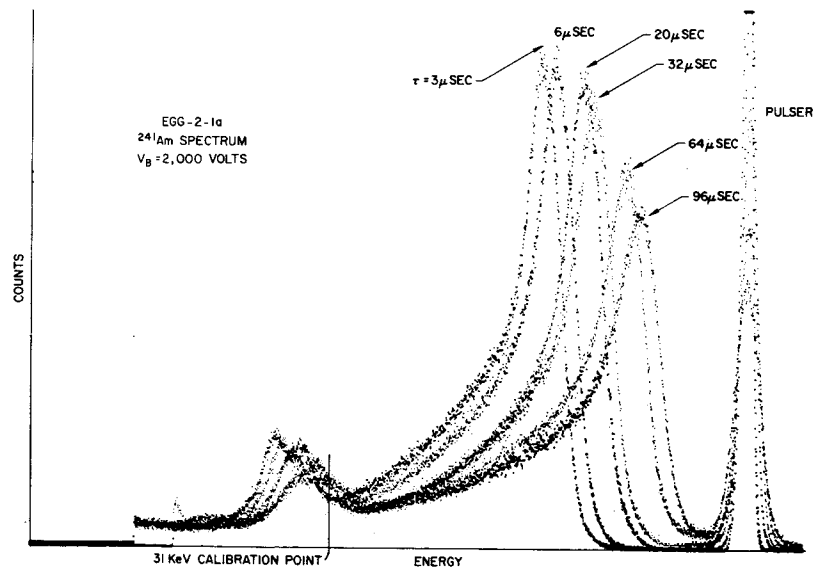


Figure 9. Effect on Spectrum of  $^{241}\text{Am}$  Source of Changing the Time Constant of a Pseudo-Gaussian Filter to very Long Values.

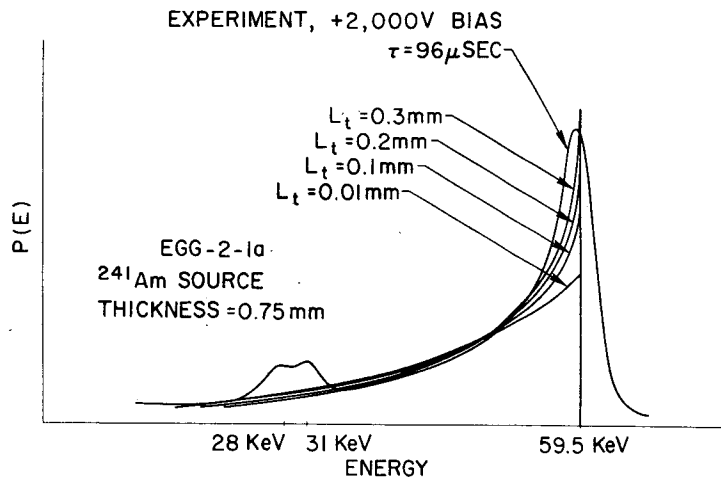


Figure 10. Calculated and Experimental Spectral Shapes for a  $\text{Hgl}_2$  Detector with Perfect Electron Collection and a Hole Trapping Length  $L_t$ .

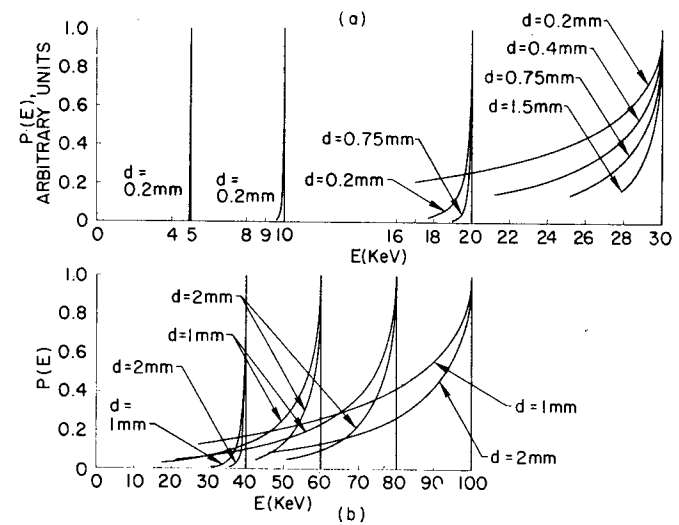
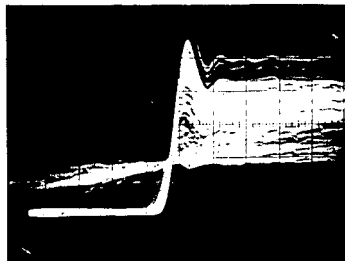


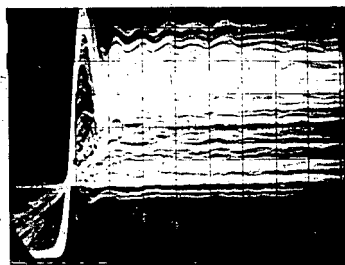
Figure 11. Calculated Spectral Shapes for  $\text{Hgl}_2$  Detectors of Different Thickness at Different Energies.  $L_t$  for Holes is 0.3 mm.

EGG-HD-1-3 ( $\alpha$ -PARTICLE EXCITATION)



ELECTRONS

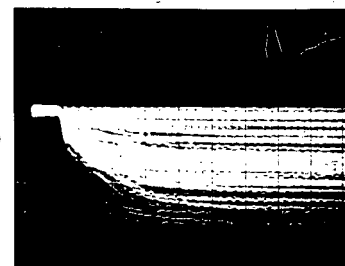
$V_B = 150$  VOLTS  
 VERT. SCALE 50 mV/DIV.  
 HOR. SCALE 20 nSEC/DIV.



$V_B = 450$  VOLTS  
 VERT. SCALE 50 mV/DIV.  
 HOR. SCALE 20 nSEC/DIV.

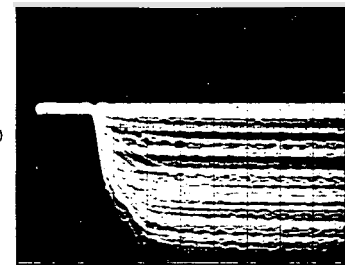
Figure 12. Response of Thin Detector to  $\alpha$ -Particle Excitation. Electron Traversal.

EGG-HD-1-3 ( $\alpha$ -PARTICLE EXCITATION)



HOLES

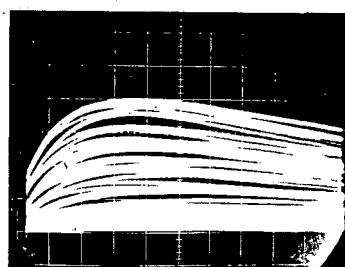
$V_B = 150$  VOLTS  
 VERT. SCALE 10 mV/DIV.  
 HOR. SCALE 100 nSEC/DIV.



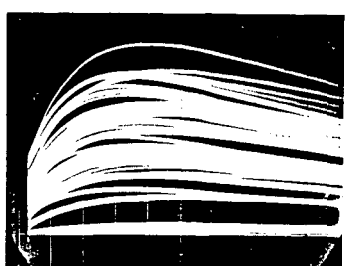
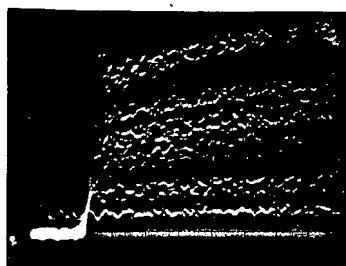
$V_B = 450$  VOLTS  
 VERT. SCALE 50 mV/DIV.  
 HOR. SCALE 50 nSEC/DIV.

Figure 13. Response of Thin Detector to  $\alpha$ -Particle Excitation. Hole Traversal.

EGG-2-1 b) ELECTRONS ( $\alpha$ -PARTICLE EXCITATION)



$V_B = 250$  VOLTS



$V_B = 1000$  VOLTS

VERT. SCALE 10 mV/DIV., HOR. 50 nSEC/DIV.

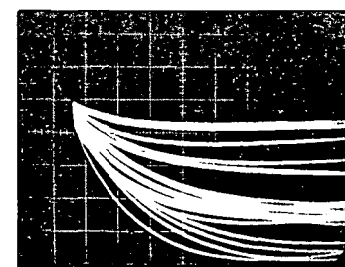
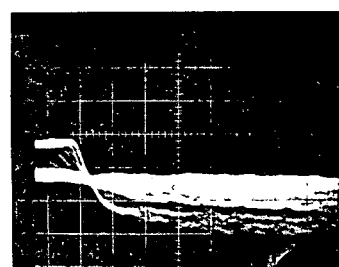
VERT. SCALE 100 mV/DIV., HOR. 20  $\mu$ SEC/DIV.

FAST PREAMPLIFIER

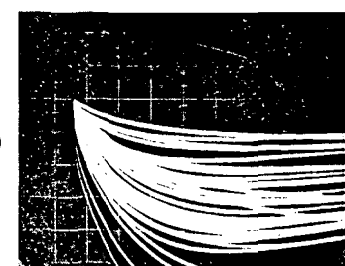
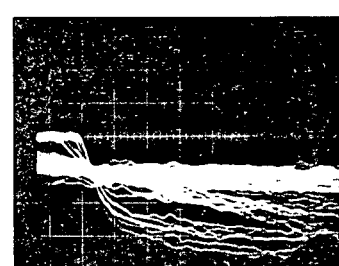
SLOW PREAMPLIFIER

Figure 14. Response of Thick Detector to  $\alpha$ -Particle Excitation. Electron Traversal.

EGG2 1 b) HOLES ( $\alpha$ -PARTICLE EXCITATION)



$V_B = 550$  VOLTS



$V_B = 1050$  VOLTS

20

H. R.

SLOW PREAMPLIFIER

Figure 15. Response of Thick Detector to  $\alpha$ -Particle Excitation. Hole Traversal.